Modern Physics Letters B, Vol. 22, No. 22 (2008) 2043–2053

World Scientific
www.worldscientific.com

FORCED COATING OF POLYPROPYLENE FIBERS WITH NON-WETTING FLUIDS: THE SCALING OF THE FILM THICKNESS

E. SHIM

College of Textiles, North Carolina State University, Raleigh, NC, USA

JUNG OK PARK[*,†] and MOHAN SRINIVASARAO[*,†,‡,§,¶]

[*]*School of Polymer, Textile and Fiber Engineering,*
[†]*Center for Advanced Research on Optical Microscopy (CAROM),*
[‡]*School of Chemistry and Biochemistry,*
[§]*Center for Nonlinear Science (CNS),*
Georgia Institute of Technology, Atlanta, GA, USA
[¶]*mohan747@ptfe.gatech.edu*

Received 27 December 2007
Revised 7 February 2008

The film thickness of free-meniscus coating of a polymeric fiber with a non-wetting fluid was investigated. A polypropylene monofilament fiber was coated with various glycerol/water mixtures. With a small capillary number (Ca), a detectable liquid film did not form on the fiber due to the non-wettability of the fiber-liquid system. Above a certain threshold velocity, liquid was forced to wet the fiber by hydrodynamic forces, thus forming a film. However, the film thickness in this region is lower than Landau–Levich–Derjaguin (LLD) theoretical value for the wetting system. At a moderate velocity range, the film thickness increases to a value predicted either by the LLD law or White–Tallmadge (WT) model, depending on the velocity, mimicking that of the wetting system. At a higher Ca, the film thickness increases much more rapidly, deviating from any predictions, due to the inertial effect.

Keywords: Forced wetting; polypropylene fibers; film thickness; coating flows.

1. Introduction

Spin-finish application, a fiber-coating process, is one example of a liquid film coating applications in the textile industry. Spin finish is applied on a fiber by the liquid film coating process to optimize fiber processability through several processing steps towards an end product. The spin finish usually contains a mixture of lubricants, antistatic agents, wetting agents and emulsifiers that are needed to modify the surface characteristics of fibers.[1] The uniform application of a spin finish on

[¶]Corresponding author.

a fiber is considered to be essential for further processing of the fibers for various applications.

During spin-finish application, the solid-air interface is replaced by a liquid–solid interface at high velocity. Therefore, it differs from static spreading of fluids on a flat surface, because the film is formed under dynamic conditions, usually by forced wetting on a cylindrical substrate. One is basically dealing with the problem of dynamic wetting and liquid film stability on a cylindrical substrate. A fiber enters a liquid reservoir filled with a finish solution, leaving the reservoir with a certain thickness of liquid film. This annular film is not stable because the Laplace pressure of the fluid is not balanced between the inner (fiber-fluid) curvature and the outer (fluid-air) curvature, and breaks up into small droplets. This process is known as the Rayleigh Instability.[2] Therefore, the coating process can be considered in three distinct steps: dynamic wetting, film formation and film instability development.

Here, we investigate the simplest case, free-meniscus coating of a monofilament polymeric fiber, to understand the coating phenomena of non-wetting fluids like spin finishes on polymeric fibers using a series of Newtonian fluids. We focus our interest only in the film formation part, and the development of Rayleigh instability will be reported later.

2. Theoretical Background

Film formation, the second step in a coating process, is governed by the balance among the various forces acting on the receding contact line, which are the long-range force, capillary force, viscous force, inertial force and gravitational force. Material and processing parameters, including the fiber diameter, liquid viscosity, and liquid surface tension, coating velocity and applicator geometry affect the force balances and determine the thickness of the fluid film on fiber surface when the fiber leaves the liquid reservoir. Other factors affecting the film formation process include non-ideality, viscoelasticity, and anisotropy of the fluid, as well as the non-wettability and surface roughness of the fiber, to name a few.

Many theoretical studies have predicted the film thickness on fibers for both Newtonian and non-Newtonian cases. When the coating velocity is zero (static wetting), the film thickness is determined by the balance between the surface tension and the long range forces. In the static case where the velocity is zero, the film thickness, e, is determined only by the fiber dimension,[3,4]

$$e_c = a^{2/3} r^{1/3} , \tag{1}$$

where r is fiber radius, a is related to the Hamaker constant, A, and fluid surface tension, γ, as

$$a = \left(\frac{A}{6\pi\gamma} \right)^{1/2} .$$

When the coating velocity is very low, $Ca \ll 1$, the film thickness results from a balance between the viscous force which is in favor of the film formation, and the capillary force, that resists film formation. For this visco-capillary regime, the film thickness, e_l, is given by[5,6] (Landau, Levich and Derjaguin, 1942),

$$e_l = 1.34 r Ca^{2/3} . \tag{2}$$

Here, Ca is the capillary number, representing the ratio of the viscous force to the capillary force, which is defined as $Ca = \eta U/\gamma$, where η is the fluid viscosity and U is the coating velocity. This expression is valid when $e_l \ll r$. When the coating velocity is increased such that e_l is not much smaller than the fiber radius, the thickness is given by[7]

$$e = \frac{1.34 r Ca^{2/3}}{(1 - 1.34 r Ca^{2/3})} . \tag{3}$$

This is valid when $Ca < 1$.

As the coating velocity is further increased, the inertial force can no longer be neglected and the film thickness increases rapidly. In this visco-inertia regime, the Weber Number ($We = \rho U^2 r/\gamma$, where ρ is the fluid density), is used to describe the film thickness,[8]

$$e \approx \frac{e_l}{(1 - We)^{2/3}} , \tag{4}$$

where e_l is the Landau–Levich–Derjaguin thickness. The Weber number is a ratio between the dynamic pressure ($\sim \rho U^2$) over the Laplace pressure ($\sim \gamma/r$), or a measure of the importance of inertia over the surface tension.

At even larger velocities, the viscous boundary layer needs to be considered. The thickness of the boundary layer, which is proportional to $(\eta L/\rho U)^{1/2}$, is usually greater than the film thickness, while at high velocity it becomes smaller than the quantity of liquid entrained by the liquid reservoir. Here, L is the length of the liquid reservoir. In this boundary layer regime, the film thickness scales as[8]

$$e = \alpha \left(\frac{\eta L}{\rho U} \right)^{1/2} , \tag{5}$$

where $\alpha = 1.3 \pm 0.1$. The film thickness decreases with the velocity and no longer depends on the surface tension, but is limited by the geometry of the reservoir since it is fixed by the length of the bath. Practically this boundary layer regime should be relevant to most industrial coating in the velocity range of 10–100 m/s.

The above discussion is valid when the coating fluid behaves as an ideal fluid. The gravitational force is also ignored, since its influence is insignificant unless the fluid film is much thicker than the fiber dimension. In the case of real solutions, deviations are found due to deformation-dependent viscosity, surface inhomogeneity, and non-wetting condition, etc. For example, a solution containing surfactants produces thicker films.[9,10] In this case, a surface tension gradient appears in the

dynamic meniscus, inducing Marangoni flow, which makes the film thicker than the predictions. Similarly, polymer solutions lead to a thicker film, which has been attributed to the normal stress effect[11] or the elongational viscosity effect.[12] In the case of liquid crystalline fluid, also leading to thicker films, analysis using Ericksen–Leslie equations shows that Frank elasticity plays no role in increasing the coating thickness for the nematic fluid over that of isotropic fluid, while viscous anisotropy is the source of observed rescaling through the deformation-stress cross-coupling and the existence of extensional kinematics in the meniscus formation region.[13]

When the coating fluid fails to wet the fiber surface, it is expected to show dry–wet transition as the coating velocity increases. Under static conditions, the non-wetting fluid forms positive contact angle on the fiber surface, while the receding contact angle decreases with coating velocity. Eventually a film is deposited when the dynamic receding contact angle reaches zero. This film is under the action of the long range force which generally squeezes the film in the non-wetting case. Therefore, at low coating velocities, no film will be formed due to the combined effect of non-zero contact angle and the long range force. At higher coating velocities, where viscous forces can dominate the capillary and long range forces, a film will be deposited. The critical velocity above which fluid-coating occurs is mainly fixed by the material's properties.[14,15]

3. Experiments

3.1. *Materials*

Polypropylene (PP) monofilament fibers, provided by the Goulston Technologies, were used in this study. The radius of the fiber was 100 μm, determined by an optical microscope. Solutions of glycerol/water at various glycerol concentrations (0, 20, 40, 50, 60, 70, 80, 90, and 100 wt.%) were prepared to systemically vary the solution viscosity while keeping the surface tension more or less constant. We should note that these solutions are non-wetting on the PP surface and would fail to remain as a uniform film, since the surface energy of PP (about 20–25 dyn/cm) is lower than surface tensions of glycerol/water solutions used.[16]

3.2. *Measurement of the physical properties of liquids*

Viscosity of the fluids was measured using capillary viscometer (Cannon–Ubbelohde Semi-In micro, size 100, No L57) at room temperature. The surface tensions of the glycerol/water solutions were measured with a capillary method at room temperature.

The viscosity and surface tension of various glycerol/water solutions are shown in Fig. 1. As the glycerol concentration increased beyond 80 wt.%, the viscosity of the liquid increased very rapidly while the surface tension gradually decreased.

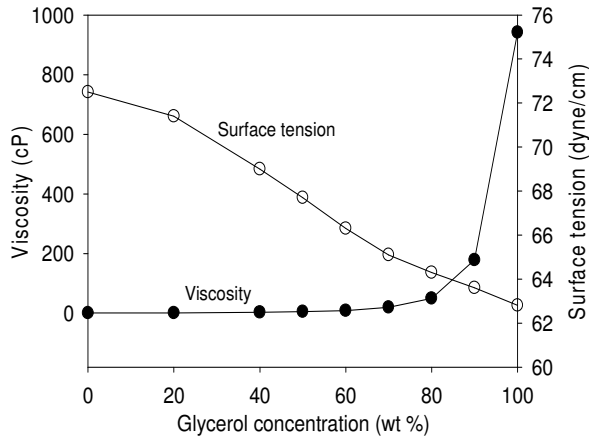

Fig. 1. Change in viscosity (•) and the surface tension (○) of glycerol/water solutions at room temperature.

3.3. *Coating process and the fluid film thickness measurement*

A fiber was horizontally withdrawn through a Teflon tube (inner diameter = 0.188 cm, length = 2.5 cm), where the fluids of interest were contained. The initial thickness of the film before break-up was measured on-line from the fluid weight picked up by the fiber at various velocities using the following relationship:

$$e = -r + \sqrt{r^2 + \frac{\Delta W/\Delta t}{\pi \rho U}}\,, \tag{6}$$

where ΔW is the amount of liquid pickup at time interval Δt.

4. Results and Discussion

When the change in the liquid weight is large enough to be measured, the rate quickly reached linearity with time. The slope of the plot increases with the withdrawal velocity (Fig. 2(a)) and the liquid viscosity (Fig. 2(b)) for each given solution. At a high velocity, the liquid is consumed so fast that the measurement quickly reached a plateau, since the amount of the fluid in the reservoir is significantly reduced during the experiment. In these cases, only the data in linear regions are used to calculate the film thickness. At an even higher velocity, the inertial effect became large and drops of liquid fell out of the liquid reservoir.

Figure 3 shows the normalized initial thickness, e/r, of glycerol/water films compiled as a function of the capillary number. Since the surface tension slowly decreases while the viscosity increases more rapidly as the glycerol concentration increases (see Fig. 1), it was required that we use higher velocities at low concentrations. The initial thickness of the film shows different trends for different solutions as expected for viscous non-ideal fluids, clearly deviating from the LLD predictions

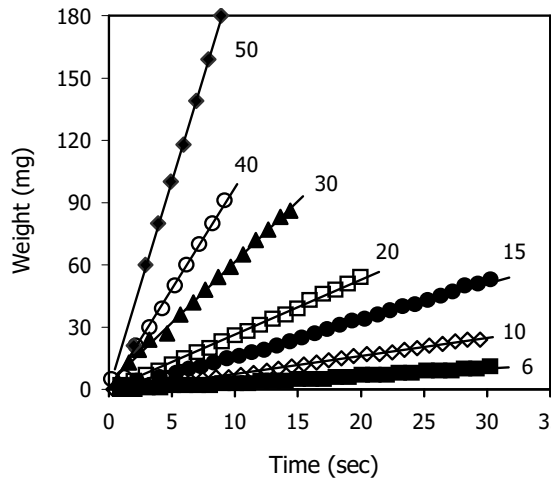

(a)

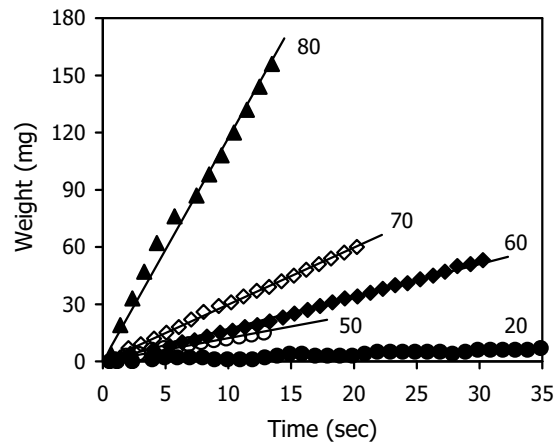

(b)

Fig. 2. Plots of the amount of the liquid picked up by the PP fiber as a function of time (a) at various coating velocities (cm/s) with 60 wt.% glycerol/water solution and (b) at various glycerol concentrations (wt.%) at the coating velocity of 15 cm/s. Some data is excluded for clearer visualization.

for inviscid ideal fluids. We discuss our findings in more detail using a series of figures that includes only 1 or 2 fluids each for better visualization. We include predictions by LLD, WT or inertial theories for comparison.

As mentioned above, a dry regime, where no film is deposited, is found at a low capillary number, especially for the low viscosity fluids. The lowest coating velocity for measurable thickness is 35 cm/s for water and 5 cm/s for 20% glycerol solution, for example. However, the exact values of critical velocity or critical capillary number above which the liquid film is deposited could not be determined because of the

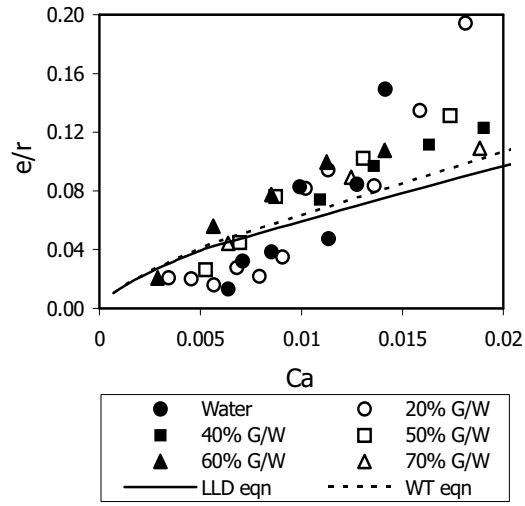

(a)

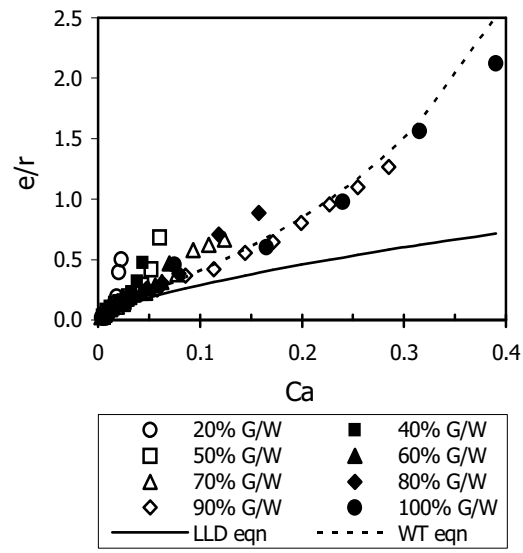

(b)

Fig. 3. Reduced film thickness, e/r, of various solutions at (a) small capillary number ranges, $Ca < 0.02$, and (b) the whole experimental range.

lack of sensitivity of the equipment. Nonetheless, it is observed that the lower the concentration of glycerol, the higher the critical velocity. Therefore, we can expect that low viscosity and high surface tension in general would lead to high critical coating velocity. Immediately after this dry–wet transition, the film formed is thinner than the LLD prediction, while the velocity range where the thickness follows

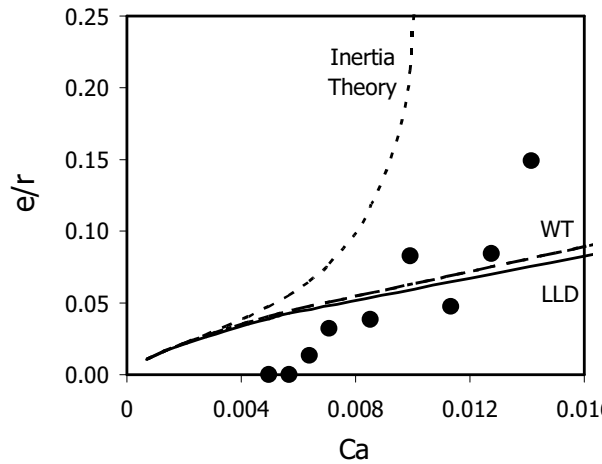

Fig. 4. The dimensionless film thickness, e/r, of water coated on the PP fiber: experimental values (•), and predictions by the inertia theory (dotted line), WT equation (broken line), and LLD equation (solid line).

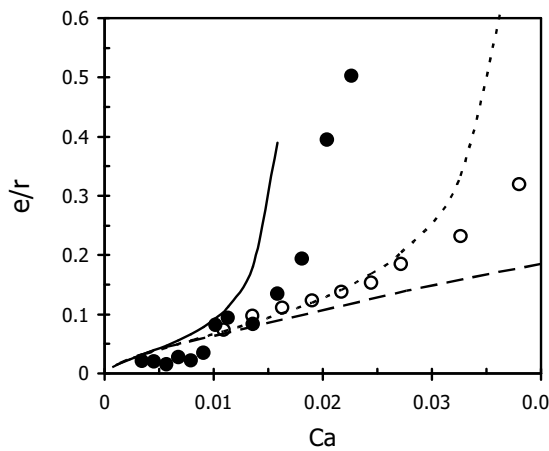

Fig. 5. The dimensionless film thickness, e/r, of glycerol/water solution coated on the PP fiber: experimental values with 20% (•) and 40% (○) glycerol content, and predictions by inertia theory for 20% (solid line) and 40% (dotted line), and WT prediction (broken line).

the LLD prediction is very narrow for the water and 20% glycerol solution (Figs. 4 and 5). Then the film thickness increases sharply above the value expected by the LLD law as the velocity increases. Inertia effect, represented by the relatively high Weber number, would be responsible for this film thickening effect. However, the experimental thickness is lower than the inertia prediction, which could be due to the non-wetting nature of our system since the prediction is for inviscid wetting solution.

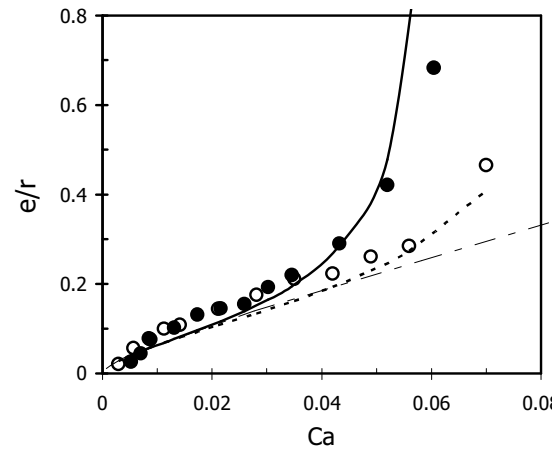

Fig. 6. The dimensionless film thickness, e/r, of glycerol/water solution coated on the PP fiber: experimental values with 50% (•) and 60% (○) glycerol content, and predictions by inertia theory for 50% (solid line) and 60% (dotted line), and WT prediction (broken line).

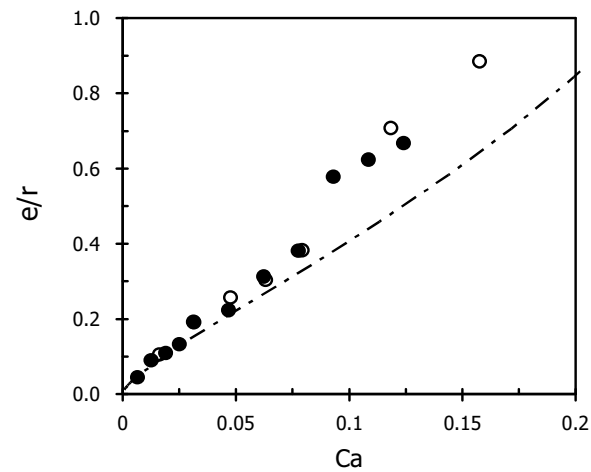

Fig. 7. The dimensionless film thickness, e/r, of glycerol/water solution coated on the PP fiber: experimental values with 70% (•) and 80% (○) glycerol content, and predicted values by the WT equation (broken line).

For the solutions of higher viscosity with glycerol content of 50% or above at intermediate capillary number and low Weber number (in the so-called visco-capillary regime), the observed value agrees reasonably well with the LLD or WT prediction (Figs. 6 and 7). Furthermore, the experimental film thickness approaches that of inertia prediction as the glycerol concentration increases from 20% to 60% (Figs. 5 and 6), which is because the effect of non-wettability is counter-balanced with the effect of higher viscosity.

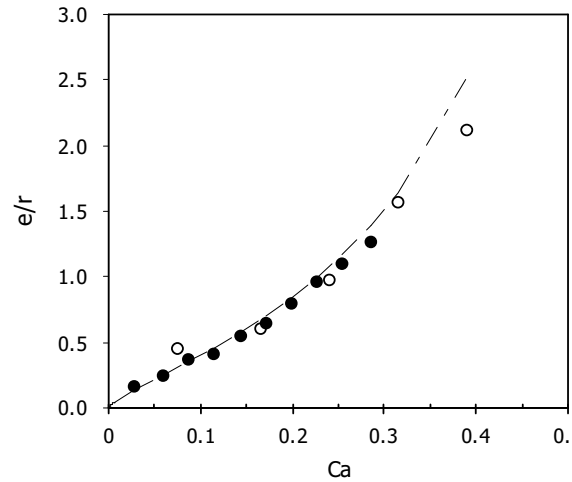

Fig. 8. The dimensionless film thickness, e/r, of glycerol/water solution coated on the PP fiber: experimental values with 90% (•) and 100% (○) glycerol content, and predicted values by the WT equation (broken line).

The film thickness with 90% and 100% glycerol solutions agrees very well with the WT expression in all experimental ranges, because their Weber numbers as well as capillary numbers fall in the ranges appropriate to the WT law (Fig. 8). For these solutions, the inertia effect is not observed within the experimental coating velocities.

5. Conclusion

We studied forced wetting of non-wetting fluids on polymeric monofilament fibers. At very low capillary numbers, no detectable film was deposited on the fiber. Above a certain Ca, a fluid film starts to form by hydrodynamic forces. However, as long as the Ca remains low, the film thickness is smaller than that of the wetting system predicted by the LLD equation. As the Ca increases, the film thickness increase to the LLD value or WT value, depending on the capillary number range, and the relation between the capillary number and the fluid film thickness becomes similar to that of the wetting system. At higher Ca, where the Weber number was not negligible, the fluid film was much thicker due to the inertial effect.

Acknowledgments

The authors acknowledge support from the National Science Foundation (NSF-DMR-0706235), and the Nonwovens Cooperative Research Center (NCRC) at the North Carolina State University.

References

1. D. Satas, *Coatings Technology Handbook* (Marcel Dekker, New York, 1991).
2. L. Rayleigh, *Proc. Roy. Soc. A* **29** (1879) 71.
3. D. Quere, *Ann. Rev. Fluid Mech.* **31** (1999) 347–384.
4. D. Quere, J. M. Dimeglio and F. Brochard-Wyart, *Revue De Physique Appliquee* **23**(6) (1988) 1023–1030.
5. L. D. Landau and B. Levich, *Acta Physicochimica USSR* **17** (1942) 42–54.
6. B. V. Derjaguin, *Acta Physicochimica USSR* **20** (1943) 349–352.
7. D. A. White and J. A. Tallmadge, *AIChE Journal* **12**(2) (1966) 333.
8. A. De Ryck and D. Quere, *J. Fluid Mech.* **311** (1996) 219–237.
9. D. Quere, A. de Ryck and O. O. Ramdane, *Europhys. Lett.* **37**(4) (1997) 305–310.
10. O. O. Ramdane and D. Quere, *Langmuir* **13**(11) (1997) 2911–2916.
11. A. de Ryck and D. Quere, *Langmuir* **14**(7) (1998) 1911–1914.
12. J. O. Park and M. Srinivasarao, Forced coating of a polymer solution on a fiber, unpublished result.
13. J. O. Park, A. D. Rey and M. Srinivasarao, *Soft Matt.* (2008), to be published.
14. R. V. Sedev and J. G. Petrov, *Colloids and Surfaces* **62**(1–2) (1992) 141–151.
15. R. V. Sedev and J. G. Petrov, *Colloids and Surfaces* **34**(2) (1988) 197–201.
16. J. Brandrup, E. H. Immergut and E. A. Grulke, *Polymer Handbook*, 4th edn. (John Wiley and Sons, New York, 1999).